Seismic Performance Evaluation of Indian code-designed Concrete Moment Resisting Frames using PBSE Procedures

Abhay Hirekhan*, Mohd. Zameeruddin and Prabhakar S. Charpe

Research Scholar, Department of Civil Engineering, Kalinga University, New Raipur Chhattisgarh, 400 019, India; hir12312@rediffmail.com

Associate Professor, Department of Civil Engineering, MGM's College of Engineering, Nanded. Maharashtra, 431 605, India; md_zameeruddin@mgmcen.ac.in

Professor, Department of Civil Engineering, Kalinga University, New Raipur Chhattisgarh, 400 019, India; prabhakar.charpe@gmail.com

Performance-based seismic design framework has provided various procedures to assessed the performance of structures exposed to seismic loads. Based on the structural and non-structural components' degree of damage, these approaches have recognized different building performance levels. The analytical compatibility of these approaches depends upon a number of parameters includes modeling of structural members, location of plastic hinges, applied lateral load patterns, effects of damping and vibration's natural period. The performance-based seismic evaluation processes described in the performance-based seismic design framework are thoroughly examined in this paper. These methods are compared for group of seventy-five reinforced concrete frames representing low, medium and high-rise structures design as per the guidelines of Indian seismic codes. Performances of these example moment-resisting frames are compared and parametric studies of engineering demand parameters are carried out. The possible gray areas for integration of performance evaluation and assessment have been put forth.

Keywords: Performance-based seismic evaluation procedures, example MRFs, pushover analysis, parametric studies

Introduction

Seismic design is a two-step process; firstly, the preliminary structural configuration is selected; followed by the evaluation of the capacity of the adopted structural configuration. If the capacity of the selected structural system meets the needed demand, then the designs are finalized. Otherwise revision in the design is done. The procedure is repeated till desired performance is reached [FEMA 445,2005; Ghobarah A., 2001 and Zameeruddin and Sangle, 2016]. Reinforced Concrete Moment Resisting Frames (RCMRFs) are commonly used for lateral load carrying systems in seismically active zones. In India, IS 1893 and IS 13920 are usually used in all states to govern seismic design and construction of RCMRFs. These codes are aimed at setting forth the basic requirements for safety of life (ductility and strength) and control of damage (serviceability drift limits) against seismic hazards. [Erduran and Yakut, 2007; Zameeruddin and Sangle, 2017a]. [Mondal, A., Ghosh, S., Reddy, G.R.,2013].

By using force-based (FBD) design requirements, which necessitate that forces and displacements remain within elastic limits, the intended outcome is achieved. When exposed to earthquakes, these structures exhibit inelastic behavior, that has been addressed by incorporating a response reduction factor to forces and displacements. Nevertheless, this indirect practice results in an incorrect assessment of the actual building response. Structures designed following these code provisions were found to get damaged or collapse during strong and moderate seismic events, thereby questioning the safety of structure and humans [Zameeruddin and Sangle, 2016; Murty et al., 2012].

Structure's seismic response is goverened by the structural components' performance to withstand earthquakes. The key components of a structural system are those which form lateral load path and vertical stability. When subjected to seismic hazards they experience inelastic incursions, which may lead towards failure of individual components or redistribution among groups of members leading to collapse of the complete structure. More than a half century, assessment of structural performance is becoming more significant in order to reflect how structures perform when subjected to seismic hazard. Primary goal of this methodology is to identify various structural performance levels. FEMA 445 has described sequential steps involved in PBSA as shown in figure 1 [FEMA 445,2006].

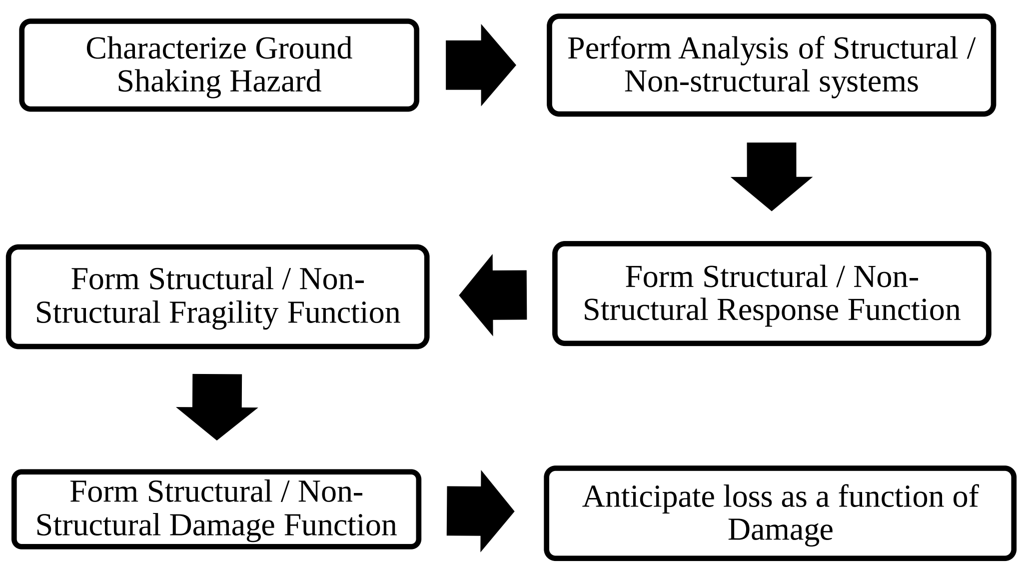

Fig.1: Performance Evaluation Process

Performance-based Seismic Assessment (PBSA) procedures use damage indices to assess the damages sustained by structure at local and global levels. These damage indices are evaluated by two approaches; (a) probabilistic and (b) deterministic. In a probabilistic method the dynamic characteristics of structures are considered. In a deterministic method various engineering demand parameter are considered to assess the state of damage. These engineering parameters include strength, stiffness, dissipated energy, curvature, deformation, base shear, stress, strain, and displacement. The damage index scales the damage value from "0" to "1," depending upon the degree of damages occurred to the structures. Where the "0" denotes no damage state and "1" denotes a collapsed state [Zameeruddin and Sangle, 2021a; Azhdary and Shabakty, 2014; Borg and Rossetto, 2010].

Performance-based Seismic Evaluation (PBSE) methodologies described in the PBSD framework assess the performance of structure based on collapse mechanism. The plastic hinges envelopes and their transition from one level of performance to the next level are represented by this collapse mechanism. The performance levels do not scale up the damage value even if they are stated as a result of damages to both structural and non-structural components. There exists an identified gray area for linking damage values with collapse mechanisms.

Performance-based Seismic Evaluation Procedures

Soft computing techniques have advanced in civil engineering, enabling researchers to undertake more complex seismic analyses with increased analysis accuracy. Two widely used PBSE approaches, the "Capacity Spectrum Method (CSM)" and the "Displacement Coefficient Method (DCM)," are presented in PBSD documentation [Boroujeni, A.R.K., 2013]. When using CSM, inelastic displacements are evaluated by comparing a structure's capacity with the demands placed on it by an earthquake's ground motion. By performing a Pushover Analysis (POA) on inelastic SDOF systems, it is possible to acquire the displacement spectra and an inelastic strength required to determine an earthquake demand. This method acknowledges that the structure’s effective period and its effective damping will increase as the structure is shaken exceeding its yield point.

It is predicted that the point at which capacity curve and demand spectrum intersect one another, exhibit the highest structural response. Performance Point is the name designated to the intersection. With this approach, the 5% damped elastic ground motion spectrum is intended to be reduced to a lower spectrum that corresponds to the structure’s response. For a particular ground motion, the structural response can be evaluated by finding the higher acceleration and displacement on the capacity curve that agrees with the ground motion requirement at the higher level of damping and longer period which the structure experiences. The approach is updated in FEMA 440. With the intention of publishing a more precise seismic evaluation, the new FEMA is presented. Figure 2 describes CSM procedure recommended in ATC 40 and FEMA 440 [Korkmaz and Irtem, 2008; Boroujeni, 2013].

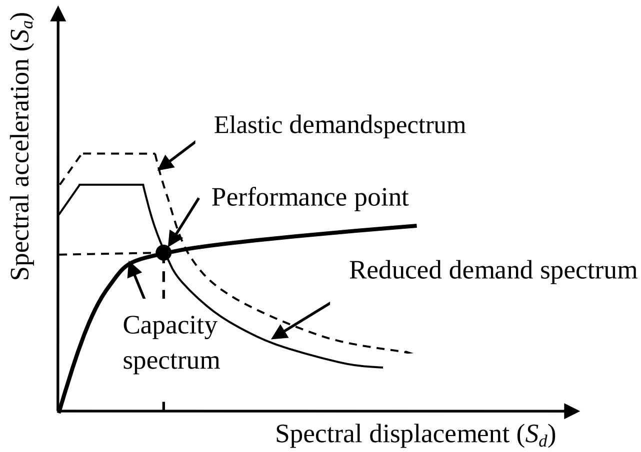

Fig. 2(a): Assessment of performance point as per ATC 40

DCM utilizes ductility to determine the highest value of displacement. The approach offers an arithmetic procedure for estimating out the displacement demand. The capacity curve does not need to be converted into spectral coordinates. The nonlinear force-displacement relationship that exists between base shear and displacement must be substituted by an idealized relationship in order to calculate the structure's effective yield strength V_y and effective lateral stiffness K_e. The bilinear aspect of this relationship is defined by an initial slope of K_e and a post-yield slope of K_s. It is necessary to select line segments on the idealized force-displacement curve using an iterative graphical method that approximately balances the area below and above the curve. Structure’s effective lateral stiffness, K_e, is considered as the secant stiffness determined at the base shear force that is equivalent to 60% of the effective yield strength V_y, of the structure. Idealized force-displacement curve is considered as a basis for the effective fundamental period in the direction under consideration. [Chopra and Goel, 2000; ASCE/SEI 41, 2007]. Figure 3 illustrated the DCM procedures described in FEMA 273 and ASCE 41.

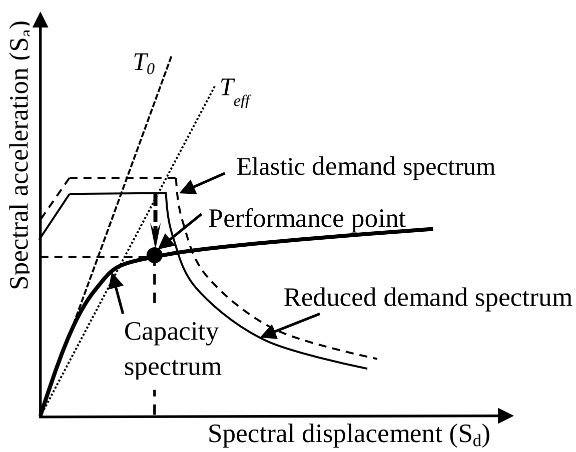

Fig 2 (b): Assessment of performance point by improved CSM

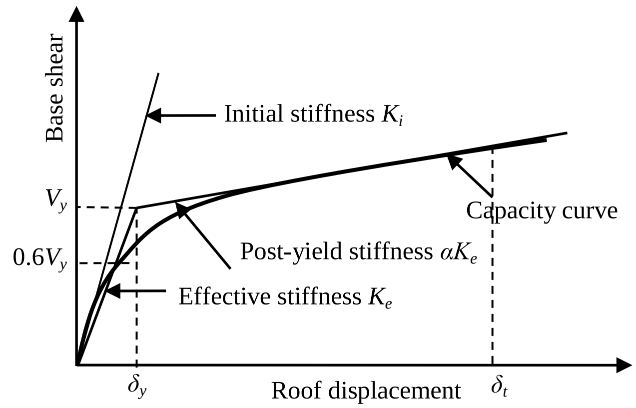

Fig. 3 (a): Calculation of target displacement as FEMA 273

All of the PBSE processes described in PBSD can give the structure's collapse mechanism, but they cannot produce any damage value on their own. In this research, an attempt has been made to acquire damage values for example MRFs subjected to lateral loads analyze for PBSE procedures. Damages are quantified using engineering demand parameters resulting in PBSE output [Zameeruddin and Sangle, 2021b]

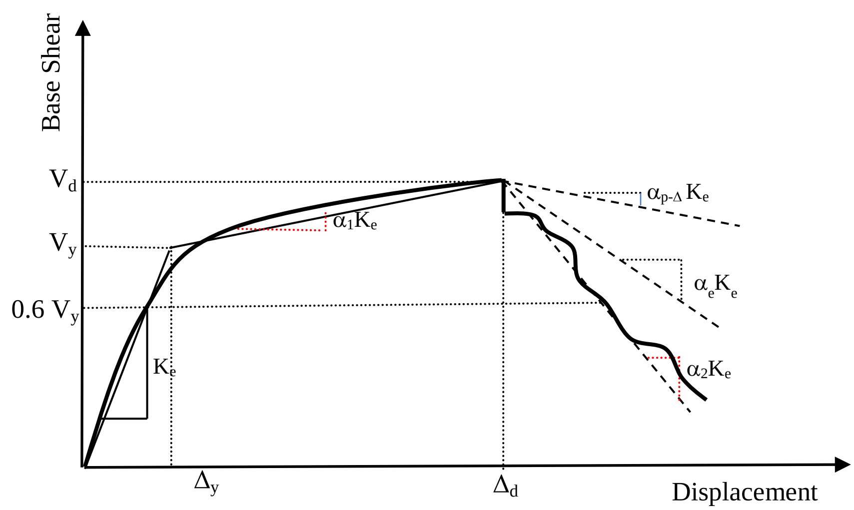

Fig. 3 (b): Idealized force–displacement curves in ASCE-41

Example RCMRFs

In this study, seventy-five example RCMRFs that represent the overall construction trend used in India have had their performance evaluated. PBSE techniques outlined in PBSD were used to assess the performance of these RCMRFs. The example RCMRFS are grouped into different categories on the basis of increasing numbers of storeys and bays. The typical bay width and storey height are both 3 m. It is believed that there are 3m between each frame. According to IS 1893, these RCMRFs depict a typical office building situated in the seismic zone "V” on a medium soil type. These RCMRFs are a representation of low, medium, and high-rise structures.

These example RCMRFs structures were analytically modelled using SAP 2000V 17.0. (Wilson and Habibullah, 2000).

The example RCMRFs structural components material characteristics are shown in Table 1 and the typical layout of the example RCMRFs is shown in Fig. 4. The design of these RCMRFs complies with the ductile detailing requirements specified in IS 456 and IS 1786 and IS 13920. Design details for structural components are given in Table 2. In Table 3, these MRFs' characteristics are listed.

The calculated demand is not the only one that can be addressed by the structural design of these RCMRFs. Several designers could propose possible approaches based on the same demand. The structural component designs used in this work were based on typical methods used by Indian engineers. For a planar frame, up to the first three storeys, all columns and beams in the story have the same section or have opted to stay the same, and then incremental changes in cross-sections are made. Design considerations taken into account the strong-column-weak-behaviors criterion.

These RCMRFs were put through a number of lateral load patterns, such as (a) the trivial lateral load pattern prescribed by IS 1893 consider as load case Push 1, (b) the uniform lateral load pattern considers as load case Push 2 and (c) the elastic first mode lateral load pattern considers as load case Push 3. Different lateral load patterns adopted in POA are displayed in Figure 5.

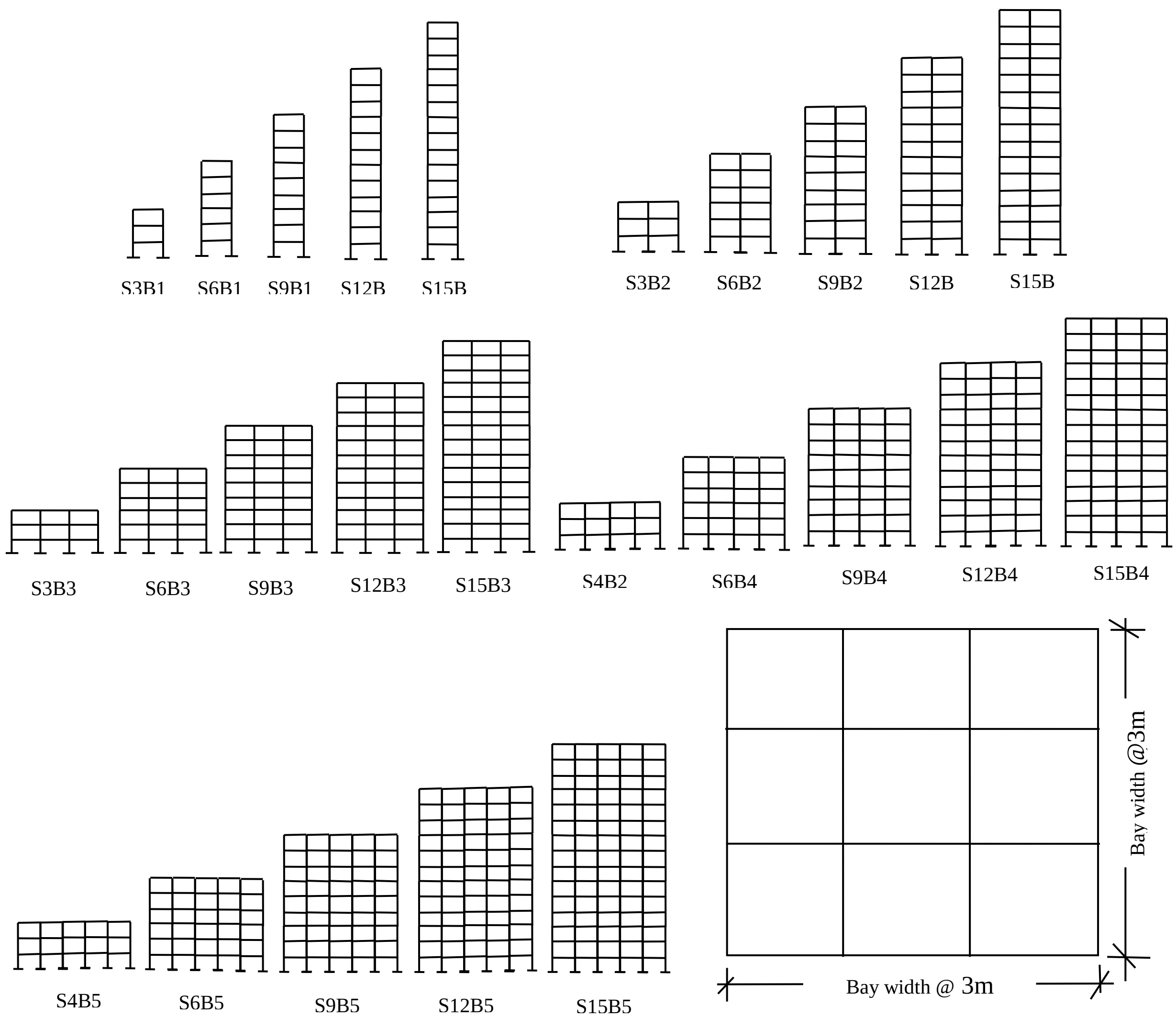

Typical Elevation (each storey of 3m c/c)

Typical Plan

Table 1: Material properties of MRFs consider for design [IS 456 and IS 1786]

Material property of MRFs	Concrete Grade, M 25	Steel Grade, Fe 415
Weight per unit volume (KN/m^3)	25	76.97
Mass per unit volume (Kg/m^3)	2.548	7.849
Modulus of elasticity (KN/m^2)	25E+ 06	2E + 08
Characteristic strength (KN/m^2)	25000	45000 (yield)
Minimum tensile strength (KN/m^2)	-	485,800
Expected yield strength (KN/m^2)	-	465,500
Expected tensile strength(KN/m^2)	-	533,500

The design base shears of RCMRFs were obtained by following the guidelines of IS 1893. The following formula is utilized for estimating a building's design base shear:

$$V_d = \frac{ZIS_a}{2Rg} W_i$$

Where; Z is 0.36 (zone factor), I is the structure's importance factor taken as 1 for these RCMRFs, R is taken as 5, W is the structure's seismic weight, and S_a is the spectral acceleration with respect to 5% damping.

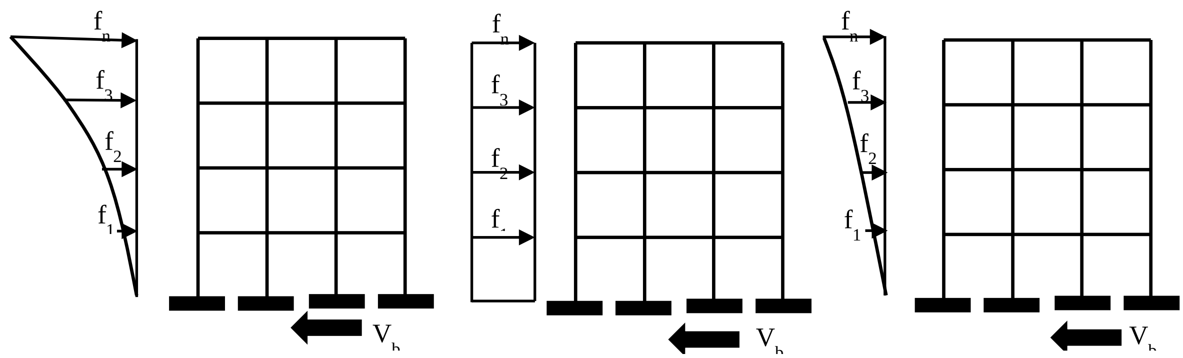

(a) IS 1893:2002 load pattern (Load case: Push 1)
(b) Uniform load pattern (Load case: Push 2)
(c) Elastic mode-1 pattern (Load case: Push 3)

Fig. 5. Different load patterns for pushover

Table 2: Details of the Reinforced Concrete section for the example RCMRFs

Group	RCMRFs	Stories	Column		Beam	
			Width (mm)	Depth (mm)	Width (mm)	Depth (mm)
I	S3B1	1 - 3	680	680	300	450
	S6B1	3 - 6	600	600	300	450
	S9B1	7 - 9	530	530	300	380
	S12B1	10 - 12	450	450	300	380
	S15B1	13 - 15	300	300	300	300
II	S3B2	1 - 3	680	680	300	450
	S6B2	3 - 6	600	600	300	450
	S9B2	7 - 9	530	530	300	380
	S12B2	10 - 12	450	450	300	380
	S15B2	13 - 15	300	300	300	300
III	S3B3	1 - 3	680	680	300	450
	S6B3	3 - 6	600	600	300	450
	S9B3	7 - 9	530	530	300	380

	S12B3	10 - 12	450	450	300	380
	S15B3	13 - 15	300	300	300	300
IV	S3B4	1 - 3	680	680	300	450
	S6B4	3 - 6	600	600	300	450
	S9B4	7 - 9	530	530	300	380
	S12B4	10 - 12	450	450	300	380
	S15B4	13 - 15	300	300	300	300
V	S3B5	1 - 3	680	680	300	450
	S6B5	3 - 6	600	600	300	450
	S9B5	7 - 9	530	530	300	380
	S12B5	10 - 12	450	450	300	380
	S15B5	13 - 15	300	300	300	300

The terms S and B specify the number of stories and bays, respectively.

Table 3: Characteristics of the studied example RCMRFs

Group	MRF	h_i (m)	T_m (S)	T_d (S)	Sa/g	W_i (kN)	V_b (kN)
I	S3B1	9	0.213	0.390	2.50	379.28	34.13
	S6B1	18	0.508	0.655	2.49	753.90	67.85
	S9B1	27	0.840	0.888	1.83	1088.04	63.40
	S12B1	36	1.225	1.102	1.48	1387.03	55.44
	S15B1	45	1.637	1.303	1.25	1630.02	48.75
II	S3B2	9	0.216	0.390	2.50	671.76	60.45
	S6B2	18	0.493	0.655	2.49	1339.92	120.59
	S9B2	27	0.792	0.888	1.83	1945.25	120.23
	S12B2	36	1.130	1.102	1.48	2497.68	108.22
	S15B2	45	1.495	1.303	1.25	2963.40	97.07
III	S3B3	9	0.217	0.390	2.50	964.30	86.78
	S6B3	18	0.488	0.655	2.49	1926.05	173.34
	S8B3	**24**	**0.674**	**0.813**	**2.03**	**2510.32**	**182.42**
	S9B3	27	0.776	0.888	1.83	2802.46	176.85
	S12B3	36	1.097	1.102	1.48	3608.33	161.09
	S15B3	45	1.443	1.303	1.25	4296.79	145.75
IV	S3B4	9	0.217	0.390	2.50	1256.84	113.11

	S6B4	18	0.485	0.655	2.49	2512.18	226.09
	S9B4	27	0.768	0.888	1.83	3659.67	233.34
	S12B4	36	1.080	1.102	1.48	4718.98	213.84
	S15B4	45	1.418	1.303	1.25	5630.18	194.33
V	S3B5	9	0.217	0.390	2.50	1549.38	139.44
	S6B5	18	0.484	0.655	2.49	3098.31	278.84
	S9B5	27	0.763	0.888	1.83	4516.88	289.77
	S12B5	36	1.071	1.102	1.48	5829.64	266.50
	S15B5	45	1.404	1.303	1.25	6963.57	242.83

Pushover Analysis

POA is performed in two steps: (i) RCMRFs are subjected to gravity loads with a load case of dead loads plus 50percent live loads (force-control), and (ii) the structure's state from the first step is recalled and subjected to a pattern of lateral loads applied to a structure with a controlled displacement of 4% corresponding to the structure's height (displacement-control). A dead load of intensity 18 kN/m and a live load of intensity 4.5 kN/m were applied to all floors. The results of the S8B3 RCMRF are discussed in detail among the seventy-five example RCMRFs. The lateral forces of S8B3 RCMRFs are summarized in Table 4.

Table 4: Lateral loads acting on the example S8B3 RCMRF

Story level	Story height (m)	Story weight (kN)	$\boldsymbol{W_i h_i^2}$	$\boldsymbol{Q_i = V_b \frac{W_i h_i^2}{\sum W_i h_i^2}}$ (kN)	Obtained from SAP 2000
Roof	24	2510.32	263775261.9	75.501	46.205
7th floor	21	2218.18	183787000.3	52.606	44.979
6th floor	18	1926.04	108173512.1	30.963	34.922
5th floor	15	1605.46	52194758.46	14.94	25.183
4th floor	12	1284.88	21395842.32	6.124	16.117
3rd floor	9	964.29	6778756.91	1.940	9.500
2nd floor	6	613.01	1217493.54	0.348	4.415
1st floor	3	281.95	2537.604	0.0007	1.104

The equivalent static method (IS 1893) and SAP yield nearly equal base shear. According to IS 1893, the lateral load distribution is a trivial load pattern, with lateral load expanding with storey height. The SAP results demonstrate the normalization of lateral loads along the building's height. These discrepancies may be accounted for by the incorporation of higher mode effects. This is the reason why we used 3 distinct load patterns to obtain both lower and upper bound values for example RCMRFs.

The moment-curvature (M-θ) behavior of the RCMRFs' members plays a major role in determining their nonlinear behavior. The moment-rotation (M-θ) relationship in SAP 2000 is necessary for nonlinear modelling in place of the moment-curvature relationship. The software's built-in stress-strain relationship, FEMA 356, was used to generate the default hinge's M-θ curve.

The contra-flexure point is often found in the middle of the members in an RCMRF with lateral loads. In a lumped plasticity model, several researchers think that plastic hinge generation at both ends of the member is best suited for POA. In the current study, concentrated M3 and P-M3 plastic hinges are integrated at both ends of the beams and columns. Figure 6 shows the acceptance standards for maximum rotational capacity, symbolized by the letters IO, LS, and CP. The modelling parameters and numerical acceptability standards are provided in Tables 5 and 6. These factors are affected by sectional characteristics like area of cross-section, percentage of rebar in compression and tension, design axial loads and design shear strength.

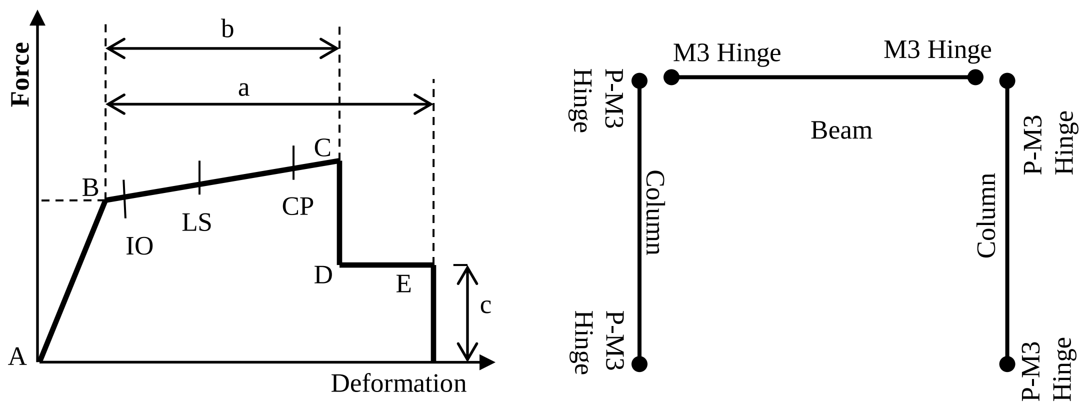

(a) Deformation control (flexure failure)

(b) Location of hinges

Fig. 5: Idealized inelastic force–deformation relationship

Table 5: Modelling parameters and numerical acceptability standards for RC beams

Conditions			**Modeling Parameters**			**Acceptance Criteria**				
			Plastic rotation angle (radians)		Residual strength ratio	Plastic rotation angle (radians)				
						Performance level				
$\frac{\rho - \rho'}{\rho_{bal}}$	Trans. Reinf.	$\frac{V}{b_w d \sqrt{f_c'}}$				IO	Component type			
							Primary		Secondary	
			A	b	c		LS	CP	LS	CP
≤ 0.0	C	≤ 3	0.025	0.05	0.2	0.010	0.020	0.025	0.02	0.05
≥ 0.5	C	≥ 3	0.020	0.03	0.2	0.005	0.010	0.02	0.02	0.03

Table 6: Modelling parameters and numerical acceptability standards for RC columns

Conditions			Modeling Parameters			Acceptance Criteria				
			Plastic rotation angle (radians)		Residual strength ratio	Plastic rotation angle (radians)				
						Performance level				
$\frac{P}{A_g f'_c}$	Trans. Reinf.	$\frac{V}{b_w d \sqrt{f'_c}}$				IO	Component type			
							Primary		Secondary	
			A	b	c		LS	CP	LS	CP
≤ 0.1	C	≤ 3	0.02	0.03	0.2	0.005	0.015	0.02	0.02	0.03
≥ 0.40	C	≥ 3	0.015	0.025	0.2	0.003	0.012	0.015	0.0 18	0.025

The responses of the example RCMRFs were studied with respect to fundamental period of vibration, roof displacement, base shear and story displacement. Using the empirical equation provided in IS 1893 for buildings without infills, the natural period of vibration was calculated. Table 3 provides the modal characteristics of each example RCMRFs.

Modal analysis of the example RCMRFs using Eigenvalues was carried out to find the fundamental period of vibration; the outcomes are shown in Table 3. The longest modal time period of vibration in the first mode is the fundamental period. The numbers that were determined utilizing code empirical relation and the basic period found using Eigenvalue analysis is virtually identical. The modal time period difference decreases as bay width increases. We can therefore draw the conclusion that the seismic code makes conservative design assumptions since it underestimates the natural duration of vibration.

Capacity curve, a plot between rooftop displacement and base shear, is used to represent the POA result. Table 7 displays base shear and rooftop displacement of example RCMRFs at the performance point for different load patterns. The engineering demand parameters, namely strength, stiffness, and ductility, generated from POA, are used in parametric to examine the seismic behavior of these RCMRFs. The pushover findings of the S8B3 RCMRF are extensively discussed for illustration purposes. The pushover curve of the S8B3 RCMRF is illustrated in Figure 6 for different loading patterns.

Table 7: Base shear and displacement of the example RCMRFs for different lateral load patterns

Push Load Case	Group	Example RCMRFs	PBSE Procedures							
			ATC 40 (CSM)		FEMA 440 (CSM)		FEMA356 (DCM)		FEMA 440 (DCM)	
			V	D	V	D	V	D	V	D
PUSH 1	I	**S3B1**	175.14	0.021	201.98	0.03	196.50	0.026	202.62	0.038
		S6B1	131.81	0.09	142.23	0.109	142.43	0.133	142.61	0.203
		S9B1	92.24	0.164	93.72	0.173	99.76	0.211	107.31	0.262
		S12B1	74.17	0.236	73.82	0.229	78.28	0.315	78.28	0.315
		S15B1	57.20	0.317	55.60	0.267	59.57	0.403	59.57	0.403

	II	**S3B2**	299.64	0.021	333.44	0.03	330.73	0.026	334.39	0.038
		S6B2	232.18	0.088	243.06	0.101	246.05	0.127	246.24	0.200
		S9B2	168.16	0.157	168.02	0.156	178.95	0.202	190.19	0.252
		S12B2	137.21	0.221	134.12	0.2	143.01	0.279	143.01	0.279
		S15B2	106.23	0.302	103.51	0.239	109.22	0.375	109.22	0.375
	III	**S3B3**	419.99	0.021	460.93	0.03	460.22	0.026	462.20	0.037
		S6B3	332.31	0.087	343.33	0.097	347.24	0.126	347.46	0.197
		S9B3	244.17	0.154	243.12	0.151	257.89	0.198	272.90	0.247
		S12B3	198.92	0.217	193.29	0.19	208.03	0.256	208.03	0.265
		S15B3	155.36	0.297	151.63	0.228	158.59	0.358	158.59	0.358
	IV	**S3B4**	546.21	0.021	596.14	0.03	595.31	0.026	597.84	0.037
		S6B4	433.84	0.087	449.25	0.097	452.01	0.124	452.94	0.195
		S9B4	320.23	0.153	318.34	0.148	336.49	0.195	355.17	0.244
		S12B4	260.37	0.215	252.36	0.184	270.27	0.255	270.27	0.255
		S15B4	204.44	0.294	199.76	0.222	207.95	0.349	207.94	0.349
	V	**S3B5**	670.38	0.021	727.64	0.03	726.67	0.026	729.73	0.038
		S6B5	534.70	0.086	552.83	0.097	556.26	0.123	556.58	0.193
		S9B5	396.31	0.152	393.68	0.147	414.26	0.191	437.93	0.242
		S12B5	321.86	0.214	310.98	0.18	332.94	0.251	332.94	0.251
		S15B5	253.63	0.292	248.06	0.219	257.56	0.345	257.56	0.345
PUSH 2	I	**S3B1**	208.49	0.011	240.35	0.015	259.85	0.018	287.39	0.023
		S6B1	201.27	0.065	210.12	0.076	210.40	0.098	210.75	0.125
		S9B1	152.65	0.111	157.28	0.128	168.61	0.171	168.73	0.208
		S12B1	121.23	0.158	123.62	0.169	134.33	0.218	134.33	0.218
		S15B1	100.20	0.209	99.68	0.202	105.93	0.287	105.93	0.287
	II	**S3B2**	368.04	0.012	418.56	0.016	443.23	0.018	467.85	0.023
		S6B2	357.47	0.063	360.05	0.07	360.50	0.094	360.52	0.12
		S9B2	275.42	0.106	286.22	0.122	298.86	0.161	297.83	0.197
		S12B2	218.35	0.153	218.52	0.153	236.19	0.206	246.34	0.239
		S15B2	183.69	0.202	180.58	0.183	191.84	0.272	191.84	0.272
	III	**S3B3**	525.53	0.012	597.33	0.016	625.72	0.018	640.37	0.023
		S6B3	507.47	0.062	507.58	0.067	508.16	0.093	507.97	0.118
		S9B3	396.29	0.105	409.81	0.118	425.35	0.155	424.01	0.192
		S12B3	314.91	0.151	313.33	0.148	337.27	0.2	351.31	0.233
		S15B3	266.26	0.199	260.44	0.176	277.24	0.262	277.24	0.262
	IV	**S3B4**	693.13	0.012	768.67	0.016	813.25	0.018	829.64	0.023
		S6B4	658.82	0.062	658.94	0.066	659.66	0.092	660.40	0.118
		S9B4	516.06	0.104	533.07	0.117	551.87	0.151	549.77	0.189
		S12B4	411.58	0.15	408.22	0.145	438.06	0.196	456.08	0.23

		S15B4	348.41	0.198	340.50	0.173	362.48	0.254	362.48	0.254
	V	**S3B5**	854.16	0.012	946.60	0.016	998.74	0.019	1010.94	0.023
		S6B5	810.27	0.061	810.41	0.065	810.80	0.091	810.83	0.117
		S9B5	636.16	0.104	656.91	0.116	679.29	0.149	677.95	0.187
		S12B5	507.76	0.15	503.55	0.145	538.78	0.194	560.73	0.228
		S15B5	430.54	0.197	420.18	0.17	446.22	0.246	446.22	0.246
PUSH 3	I	**S3B1**	179.19	0.018	213.66	0.025	208.47	0.024	216.73	0.034
		S6B1	146.44	0.083	155.80	0.099	156.06	0.126	156.21	0.186
		S9B1	103.99	0.15	106.60	0.164	113.45	0.203	121.15	0.25
		S12B1	82.97	0.216	83.34	0.219	87.25	0.28	87.25	0.28
		S15B1	62.63	0.298	61.18	0.257	66.52	0.38	65.52	0.38
	II	**S3B2**	308.65	0.018	357.99	0.027	353.20	0.024	358.82	0.033
		S6B2	261.67	0.08	271.46	0.091	271.84	0.119	271.89	0.175
		S9B2	193.20	0.142	195.28	0.149	207.35	0.194	218.18	0.237
		S12B2	152.82	0.203	150.56	0.192	161.98	0.255	161.98	0.255
		S15B2	117.90	0.282	115.14	0.228	121.17	0.351	121.17	0.351
	III	**S3B3**	439.15	0.018	497.26	0.026	496.73	0.024	498.56	0.033
		S6B3	377.38	0.079	384.98	0.087	385.09	0.118	385.32	0.172
		S9B3	282.49	0.139	284.68	0.145	300.50	0.188	315.09	0.233
		S12B3	222.39	0.199	217.45	0.182	233.96	0.245	233.96	0.245
		S15B3	173.40	0.276	169.26	0.217	177.00	0.336	177.00	0.336
	IV	**S3B4**	570.56	0.018	643.95	0.026	643.39	0.024	645.59	0.033
		S6B4	494.26	0.079	502.45	0.087	502.60	0.117	502.88	0.17
		S9B4	371.92	0.137	373.95	0.141	392.61	0.183	408.30	0.229
		S12B4	291.63	0.197	284.27	0.177	304.60	0.236	304.60	0.236
		S15B4	228.93	0.273	223.42	0.211	232.81	0.327	232.81	0.327
	V	**S3B5**	701.79	0.018	786.77	0.026	786.14	0.024	788.78	0.033
		S6B5	610.81	0.079	617.63	0.085	617.74	0.116	618.13	0.169
		S9B5	460.73	0.131	459.96	0.12	463.54	0.168	466.89	0.212
		S12B5	360.79	0.196	351.18	0.174	375.33	0.231	375.33	0.231
		S15B5	284.29	0.271	277.51	0.208	288.40	0.319	288.40	0.319

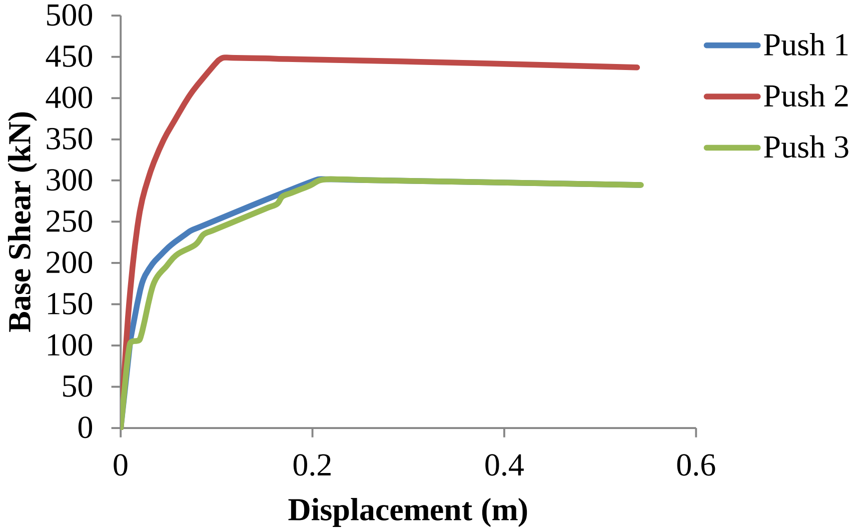

Fig. 6: Pushover curve of S8B3 RCMRF for three distinct lateral load patterns

The base shear and displacement at performance point serve to describe the nonlinear properties of the example RCMRFs. According to the analysis of the S8B3 capacity curve, the Push 2 load case demonstrated a force-controlled mechanism, while the Push 1 load case described a displacement-controlled system. Therefore, a set of lateral loads must be applied to evaluate the effects of lateral loads on an example RCMRF. Table 8 provides the base shear and displacement at a performance point for example S8B3 RCMRF. Pushover curve of all example RCMRFs is shown in Figure 7 (a) – (o).

Table 8: Values of base shear and displacement at performance point of example S8B3 RCMRF

Example RCMRF S8B3	ATC 40 (CSM)		FEMA 440 (CSM)		FEMA 356 (DCM)		FEMA 440 (DCM)	
	V	D	V	D	V	D	V	D
Push 1	267.17	0.131	268.79	0.135	286.92	0.173	301.38	0.225
Push 2	430.33	0.09	447.01	0.104	448.35	0.14	446.90	0.192
Push 3	308.61	0.118	313.77	0.128	334.04	0.166	334.67	0.21

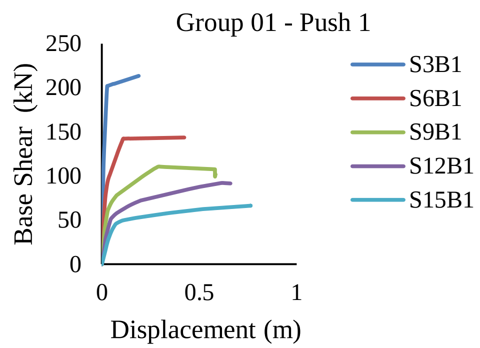

(a) Pushover Curve 0f Group I RCMRFs

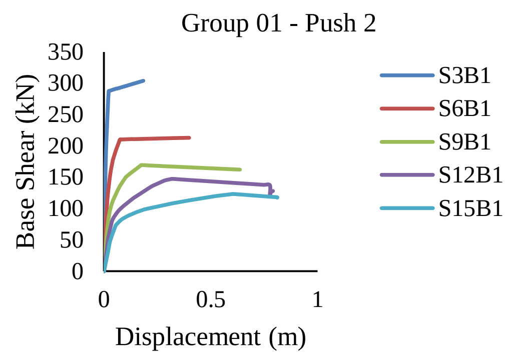

(b) Pushover Curve 0f Group I RCMRFs

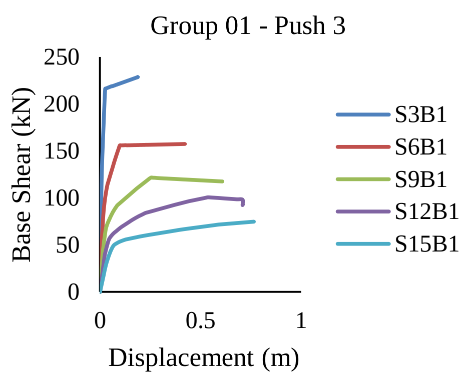

(c) Pushover Curve Of Group I RCMRFs

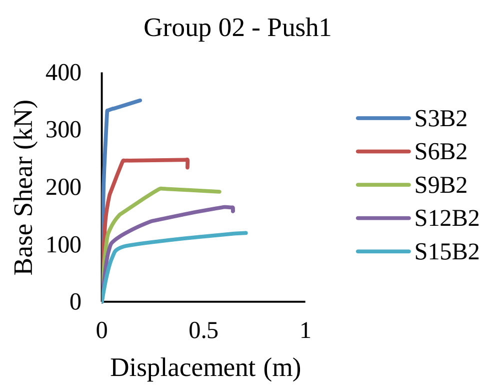

(d) Pushover Curve Of Group II RCMRFs

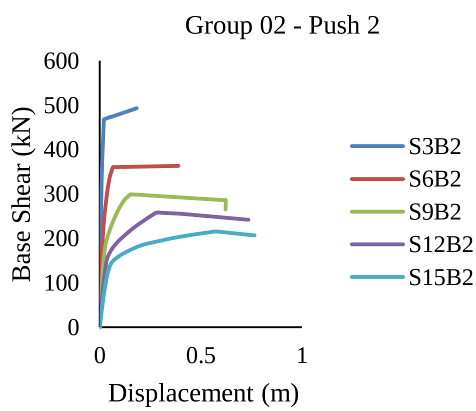

(e) Pushover Curve Of Group II RCMRFs

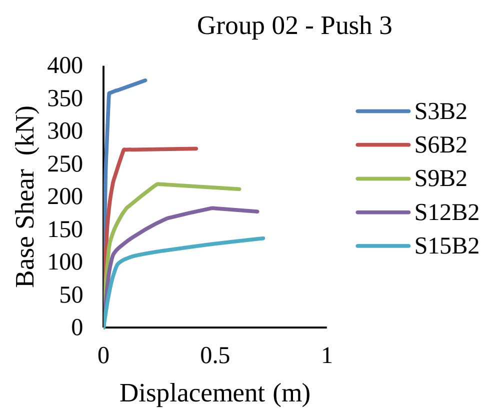

(f) Pushover Curve Of Group II RCMRFs

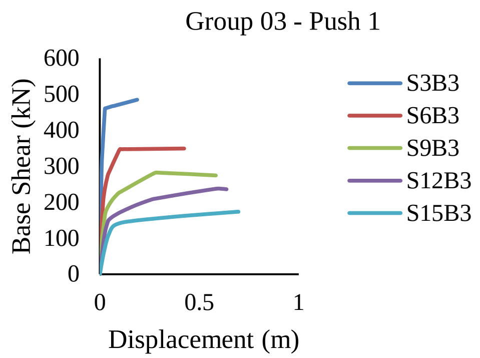

(g) Pushover Curve Of Group III RCMRFs

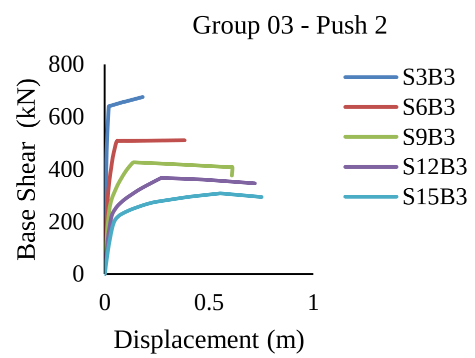

(h) Pushover Curve Of Group III RCMRFs

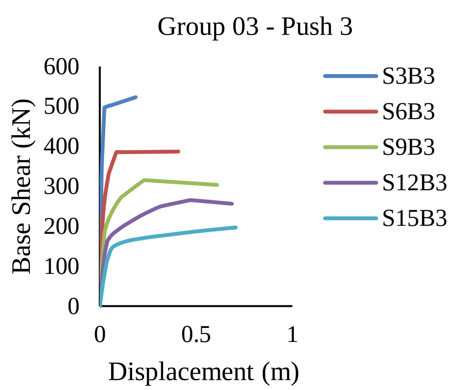

(i) Pushover Curve Of Group III RCMRFs

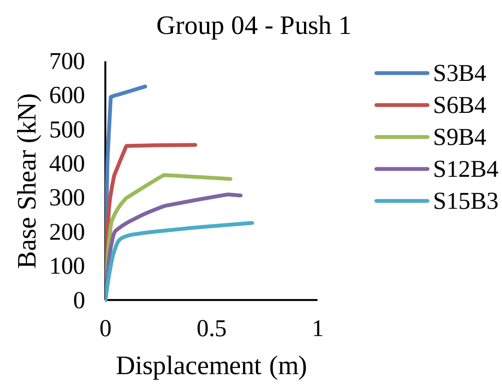

(j) Pushover Curve Of Group IV RCMRFs

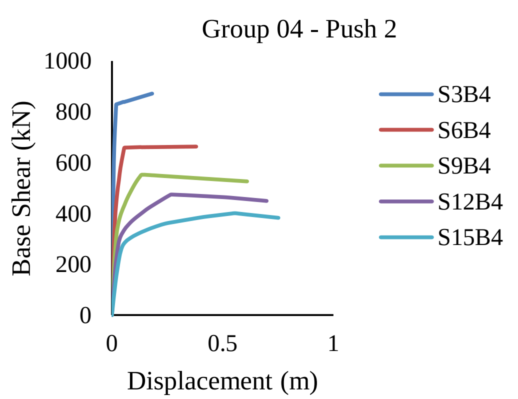

(k) Pushover Curve Of Group IV RCMRFs

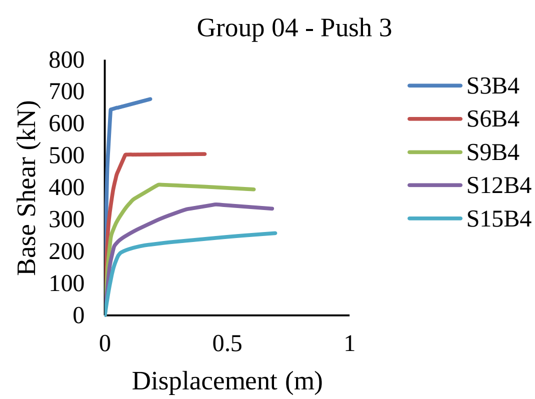

(l) Pushover Curve Of Group V RCMRFs

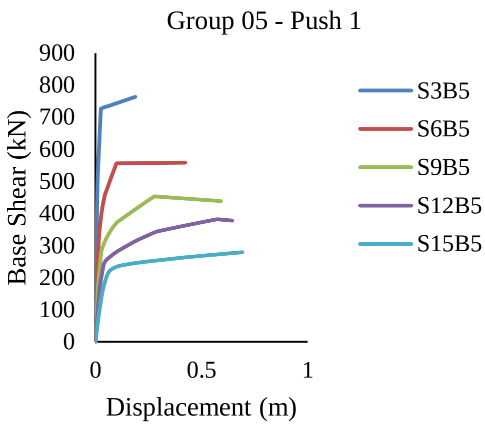

(m) Pushover Curve Of Group V RCMRFs

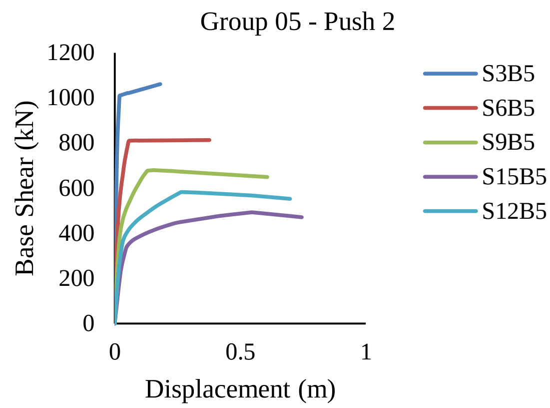

(n) Pushover Curve Of Group V RCMRFs

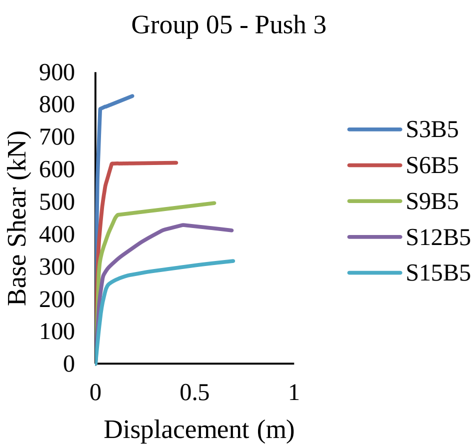

(o) Pushover Curve Of Group V RCMRFs

Fig. 7: Pushover curve of all example RCMRFs for three distinct lateral load patterns

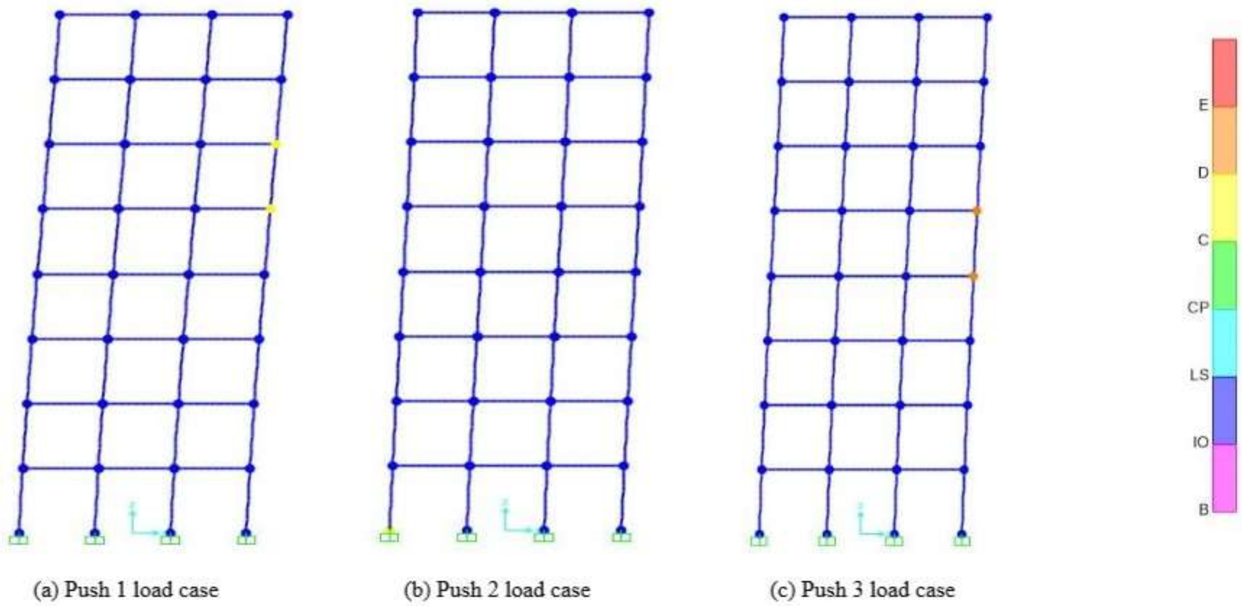

Fig. 8: Collapse Mechanism of the plastic hinges in Example S8B3 RCMRF

The initial slopes of the capacity curve describe the structural components of the RCMRF that have been damaged. The RCMRF initial slope in the load case Push 2 for S8B3 is higher than that in the load case Push 1.

This might be a result of plastic hinges yield mechanism. In the load case Push 2, damages concentrate in the upper storeys (in the beams only) for larger values of displacement, whereas in the load case Push 1, damages are concentrated in the lower storeys (in the columns). Consequently, it can be said that push 1's load case is force-controlled**.** Figure 8 describes the collapse mechanism of S8B3 RCMRF. Table 9 gives initial stiffness of S8B3 RCMRF subjected to different loading condition.

In PBSD performance of a structure is defined by discrete levels namely Operation level (OP), Immediate Occupancy (IO), Life Safety range (LS), Collapse Prevention level (CP) and Collapse (C). These are identified based on damages to structural and non-structural components. Table 10 shows the permissible limits of drift and obtained drift of S8B3 RCMRF.

Table 9: Values of initial stiffness for example S8B3 RCMRF for different load patterns

Example S8B3 RCMRF	Initial Stiffness (kN/m)
PUSH 01	10571.6
PUSH 02	17252.9
PUSH 03	12134.5

Table 10: Permissible limits of drift and obtained drift of S8B3 RCMRF

Performance levels	Drift Value

	Prescribed value (%)	Obtained value (%)		
		Push 1	Push 2	Push 3
Operational level	< 0.7	0.040	0.036	0.039
Immediate occupancy level	1	0.042	0.036	0.039
Life safety level	2	0.784	0.886	0.822
Collapse prevention level	4	2.256	2.243	2.300
Collapse	> 4	2.256	2.243	2.300

In POA lateral loads are applied incrementally, in each incremental step of POA there is increase in lateral drift. The attainment of a damage state is identified by the permissible limits of drift as described in FEMA. Table 10 provides the details of drift of S8B3 RCMRF at identified performance levels. These performance levels have been traced with reference to formation of plastic hinges (both in beams and columns) and their transition from one performance level to other.

The formation of first hinge is considered to be attainment of operational level (OP). later sequence of shift of this plastic hinge are used to accumulate the responses in other performance levels. It has been observed that during a POA there is a fall in strength and stiffness at each incremental step. Table 11 provides the displacement, base shear and stiffness at identified performance levels of S8B3 RCMRF.

Table 11: Displacement, Base shear and Stiffness at identified performance level of S8B3 MRF

Performance levels	Push 1			Push 2			Push 3		
	Displacement (m)	Base Shear (kN)	Stiffness (kN/m)	Displacement (m)	Base Shear (kN)	Stiffness (kN/m)	Displacement (m)	Base Shear (kN)	Stiffness (kN/m)
Operational level	0.01	101.49	10571.56	0.01	151.36	17252.94	0.01	115.22	12134.49
Immediate occupancy level	0.01	107.62	10571.61	0.01	151.36	17252.94	0.01	115.22	12134.49
Life safety level	0.19	293.92	1561.01	0.21	446.41	2098.62	0.20	334.86	1696.55
Collapse prevention level	0.54	294.59	543.99	0.54	437.16	811.97	0.55	327.52	593.35
Collapse	0.54	294.59	543.99	0.54	437.16	811.97	0.55	327.52	593.35

PBSE procedures are useful to identify the collapse mechanism through the formation of plastic hinges. One can attempt to scale the damage state of the structure using this collapse mechanism. The engineering demand parameters such as storey drift, inter-storey drift, base shear and derived quantities such as ductility, stiffness and energy dissipated can be used to form a damage indicator.

Many attempts have been made in past to scale these damages. The document damage indicators in available literature as calibrated using nonlinear dynamic analysis. These efforts have result in affirmative way of damage assessment but follows the limitation computational effort, hence not found common in practice. Some researchers have provided damage assessment indices using nonlinear static methods but followed the limitation of POA to address the inelastic excursion. This demand a rational approach of damage assessment integrated with PBSE which will help designer to identify attainment of performance level with a damage value. Such an attempt will help designers to follow the frameworks of next-generation PBSD with identified performance levels in terms of repair, downtime and casualties. The scope of the present study is to understand the available PBSE procedures and identify the gray areas towards integration of PBSE with damage assessment.

Conclusion:

Studies have been done on various performance-based seismic evaluation techniques that are listed in PBSD. For this, 75 force-based design RCMRFs were put under various lateral loads, and a parametric research was conducted to investigate the performance levels of the buildings. The chosen frames show how low-rise, medium-rise, and high-rise building designs and construction techniques are generally applied throughout the Indian subcontinent.

The arrangement of the sample RCMRFs used to demonstrate these consequences of an increase in storey height and bay width. A recognized class of structures is represented by the groupings of example RCMRFs. Understanding the local and global behavior of example RCMRFs exposed to pre-defined seismic risks is made easier by the use of PBSE methods on the example RCMRFs. In order to determine the envelope of top bound and lower bound values of inelastic intrusions, various lateral load patterns were applied to example RCMRFs.

These envelopes were useful for figuring out the causes of failure. The parametric research done on the example RCMRFs demonstrated the potential of merging the PBSE with the attainment of a damage value that is required in order for the PBSD to become a standard procedure in practice. The following are the conclusions from the parametric study:

- The response reduction factors for forces and displacements are used to account for inelastic effects according to current seismic design rules. However, such a deceptive strategy makes it difficult to comprehend the true building performance in a nonlinear state.
- Current seismic codes' equivalent static technique for earthquake-resistant design is insufficient to account for higher modes of vibration, leading to cautious design.
- The capacity spectrum method and displacement coefficient method are the PBSE techniques recommended in PBSD. Which approach should be utilized in practice is an issue that is raised when these methods are evaluated for the example RCMRFs and reveal various results for displacements.
- Different lateral load patterns, including the trivial lateral load pattern proposed in IS 1893, the uniformly distributed lateral load pattern, and the elastic first mode lateral load pattern, were used in POA. The envelopes of upper and lower bound values are the outcome of these lateral load patterns. As a result, a single set of lateral load patterns cannot address nonlinear behavior; but, a set of two or more lateral load patterns can examine nonlinear phenomena in greater detail.

- The collapse mechanism caused by the PBSE methods illustrates how plastic hinges form and drop from one performance level to another. These mechanisms, namely force-controlled and displacement-controlled hinges, aid in determining the type of failure based on the concentration of hinges. The positioning and modelling of plastic hinges affect the collapse mechanism. It is necessary to optimize the modelling of nonlinear hinges and their placement in order to determine the precise values of nonlinear state.
- RCMRFs exhibit a force-controlled behavior when a uniform lateral load pattern is applied. This might be caused by the columns' development of hinges for shear and bending. However, for trivial load patterns, the displacement-controlled behavior manifests because only the bending of the beams causes the formation of plastic hinges.
- The stiffness value significantly decreases during the incremental POA steps, and PBSE has utilized this to track the achievement of various performance levels. The drift criterion served as the foundation for performance levels. They can only show when a certain limit state has been reached; they cannot scale any damage values.
- The assessment of building performance levels and the likelihood of damage is required by contemporary seismic design trends. These performance levels are currently a subject of inquiry.
- Significant work has been done in the current literature to integrate the damage state with the identified performance levels. These initiatives make use of nonlinear dynamic analysis, which requires laborious and complicated computations and is therefore not frequently used by professional engineers.
- Nonlinear static analysis has been attempted to assess the damage condition, but these efforts were constrained by the POA.

The current work focuses on overcoming POA's limitations to improve damage assessment processes utilizing POA. The engineering demand parameters that resulting from POA can be used to define the damage and vulnerability indicators. The scope currently only includes parametric studies of the engineering demand parameter. Future work will include calibrating the damage or vulnerability index.

Acknowledgement

The authors of this study recognize the research contributions made by all the cited sources as well as the assistance of MGM College of engineering, Nanded, India and by the Chairman, Kalinga University, New Raipur, Chhattisgarh, India.

References

[1] Emrah Erduran and Ahmet Yakut (2007). Vulnerability Assessment of Reinforced Concrete Moment Resisting Frame Buildings. Journal of structural engineering, 133: 576-586. DOI: 10.1061/(ASCE)0733-9445(2007)133:4(576)

[2] Zameeruddin, M., Sangle, K.K., (2017a). Seismic Performance Evaluation of Reinforced Concrete Frames Subjected to Seismic Loads. Journal of Institute of Engineers, India Series A, DOI 10.1007/s40030-017-0196-0

[3] Zameeruddin, M., Sangle, K.K., (2016). Review of Recent Developments in the Performance-based Seismic Design of Reinforced Concrete Structures. Structure 6: 119-133. http://dx.doi.org/10.1016/j.istruc.2016.03.001

[4] Murty CVR, Goswami R, Vijaynarayan A. R., Mehta V.V.,(2012). Some Concepts in Earthquake Behaviour of Buildings, Gujarat State Disaster Management Authority, Government of Gujarat, India.

[5] Azhdary, F., Shabakty, N., (2014). Performance based Design and Damages Estimation of Steel Frames with Consideration of Uncertainties. Technical Gazette, 21, 351–358. UDC/UDK 624.014.2.042.7:620.191.3

[6] Borg, R.C., Rossetto, T., (2010). Performance based Seismic Design and Assessment Methodologies: relation to Damage and Requirements. 8th Fib PhD Symposium in Kgs, Lyngby, Denmark

[7] Zameeruddin M and Sangle KK (2021a). Damage Assessment of Reinforced Concrete Moment Resisting using Performance-based Seismic Evaluation Procedure. Journal of King Saud University-Engineering Sciences, 33(4):1-13. https://doi.org/10.1016/j.jksues.2020.04.010

[8] ATC-40, Seismic evaluation and retrofit of existing concrete buildings. Redwood City (CA): Applied technical council, 1996.

[9] FEMA 273, NEHRP guidelines for the seismic rehabilitation of buildings. Washington (DC): Federal emergency management agency, 1996

[10] FEMA 356. Prestandard and commentary for the seismic rehabilitation of buildings. Washington (DC): Federal emergency management agency, 2000.

[11] Korkmaz, K. A., Irtem, E.,(2008) Evaluation of previous and current performance-based analysis method. The 14th World conference on earthquake engineering, Beijing, China. http://www.iitk.ac.in/nicee/wcee/article/14_14-0046.PDF.

[12] Boroujeni, A. R. K., (2013). Evaluation of various methods of FEMA 356 compare to FEMA 440. Journal of civil engineering and construction technology, 4(2); 51-55. DOI: 10.5897/JCECT12.082

[13] Chopra, A. K., Goel, R. K., (2000). Evaluation of NSP to estimate seismic deformation: SDF system. J. Struct. Eng., 126 (4); 482–490. DOI:10.1061/(ASCE)0733-9445(2000)126:4(482)

[14] ASCE/SEI 41. American society of civil engineers. Seismic rehabilitation of existing building. Reston, Virginia, 2007.

[15] Wilson EL, Habibullah A., (2000). SAP 2000/NL-PUSH software, Computer and structures, Inc (CSI), version 17.0, Berkely (CA. USA)

[16] BIS IS 456, Indian standard plain and reinforced concrete-code of practice (fourth revision). Bureau of Indian Standards, 2000, New Delhi.

[17] BIS IS 1786, Indian Standard for high strength deformed steel bars and wires for concrete reinforcement. Bureau of Indian Standards, 2008, New Delhi.

[18] BIS IS 1893, Indian Standard criteria for earthquake resistant design of structures (part 1): general provisions and buildings (fifth revision). Bureau of Indian Standards, 2002, New Delhi.

[19] BIS IS 13920. Indian Standard ductile detailing of reinforced concrete structures subjected to seismic forces– code of practice (incorporating amendment nos. 1 and 2). Bureau of Indian Standards, 2000–03, New Delhi.

[20] FEMA 445, 2006. Next-generation performance-based seismic design guideline program for new and existing buildings. Federal Emergency Management Agency, Washington (DC).

[21] Zameeruddin, M., Sangle, K.K., (2017b). Seismic damage assessment of reinforced concrete structure using nonlinear static analyses. KSCE J. Civil Eng. 21 (4), 1319–1330. https://doi.org/10.1007/s12205-016-0541-2.

[22] Zameeruddin, M., Sangle, K.K., (2017c). Energy-based damage assessment of RCMRFs using pushover. Asian J. Civil Eng. (BHRC) 18 (7), 1077–1093.

[23] Ghobarah, A., (2001). Performance-based design in earthquake engineering: state of development. Engineering Structures, 23, pp. 878–884.
DOI: 10.1016/S0141-0296(01)00036-0

[24] Mondal A., Ghosh S., Reddy G.R., (2013). Performance-based evaluation response reduction factor for ductile RC frames. Engineering Structures, 56. Pp 1808-1819.

[25] Ghosh, S., Datta, D., Katakdhond, A.A., (2011). Estimation of the Park–Ang damage index for planar multi-storey frames using equivalent single-degree systems. Engineering Structures, 33, 2509–2524.

[26] Inel, M., and Ozmen, H.B., (2006). Effects of plastic hinge properties in nonlinear analysis of reinforced concrete buildings. Engineering Structures, 28, 1494–1502.

[27] Lagaros, N.D., Fragiadakis, M., (2011). Evaluation of ASCE-41, ATC-40 and N2 static Pushover methods based on optimally designed buildings. Soil Dynamics and Earthquake Engineering, 31, 77–90.

[28] Sasaki, K.K., Freemanand, S.A., Paret, T.F., Multi-Mode Pushover Procedure (MMP) – A method to identify the effects of higher modes in a Pushover Analysis. 6th U.S. National Conference on Earthquake Engineering.

[29] Bo-quan LIU, Ming LIU, Ying-bin LI, (2004). Research & development of Performance-Based Seismic Design Theory. 13th World Conference on Earthquake Engineering Vancouver, B.C., Canada , Paper No. 2457

[30] Fajfar, P., (1999). Capacity Spectrum Method Based On Inelastic Demand Spectra. Earthquake Engineerin and Structral Dynamics, 28, 979-993.